Received: 8 July 2021 | Revised: 24 August 2021 | Accepted: 6 September 2021

DOI: 10.1002/ldr.4092

RESEARCH ARTICLE

WILEY

Effects of Ca^{2+} on migration of dissolved organic matter in limestone soils of the southwest China karst area

Peiwen Xiao[1,2] | Baohua Xiao[1] | Muhammad Adnan[1,2]

[1]State Key Laboratory of Environmental Geochemistry, Institute of Geochemistry, Chinese Academy of Sciences, Guiyang, PR China

[2]College of Resources and Enviroment, University of Chinese Academy of Sciences, Beijing, PR China

Correspondence
Baohua Xiao, State Key Laboratory of Environmental Geochemistry, Institute of Geochemistry, Chinese Academy of Sciences, 99# West Lincheng Road, Guiyang, Guizhou 550081, PR China.
Email: xiaobaohua@mail.gyig.ac.cn

Funding information
National Natural Science Foundation of China-Guizhou Joint Fund for Karst Science Research Center, Grant/Award Number: U1612441; National Natural Science Foundation of China, Grant/Award Numbers: 41773147, 41273149

Abstract

The prospect of carbon sequestration in soils of karst areas remains unclear. The study on migration and transformation of dissolved organic matter (DOM) in limestone soil under the high calcium environment of karst regions has seldom been reported. This study conducted soil column experiments on two surface soils (H1 and S2) and two subsurface soils (H2 and S2) from two limestone soil profiles in the karst region of southwest China and investigated their DOM leaching behaviours under different Ca^{2+} concentration levels. The results showed that the DOM leaching process can be described by the Elovich equation, including a rapid DOM release stage and the relatively stable DOM release stage. When the Ca^{2+} concentration of eluent increases from 0 to 2.5 mmol L^{-1}, the percentage of dissolved organic carbon (DOC) loss in H1, H2, S1, and S2 soils decreased from 66.3% to 58.8%, from 76.2% to 72.4%, from 73.0% to 68.8%, and from 52.5% to 46.6%, respectively, and the apparent molecular weight of leached DOM increases, the aromaticity of leach DOM and the contribution of humic-like components decrease. The results further show that the influence of Ca^{2+} on easily leaching DOM is stronger than that on the stable DOM, indicating that high Ca^{2+} runoff can enrich high aromaticity and high molecular weight soil organic matter (SOM) in the limestone soil during the leaching process. This research is helpful to understand the migration and fate of SOM in limestone soils and provides theoretical support for increasing soil carbon sinks in karst areas.

KEYWORDS
calcium, dissolved organic matter, dynamic leaching process, EEM-PARAFAC, karst area, limestone soil

1 | INTRODUCTION

Soil is an important source and sink in the global carbon cycle (Batjes, 1996). The change of soil carbon pool directly affects the carbon storage and release of the ecosystem (Ramesh, et al., 2019). A basic problem in understanding the evolution of the soil carbon pool is the stability of soil organic carbon (SOC) under the changes in the ecological environment (Dash et al., 2019). Migration and transformation of SOC are the basic processes involving the fixation and stabilization of SOC (H. Y. Tang et al., 2019). In order to improve the understanding of mechanisms underlying the soil carbon sequestration, carbon-related physical–chemical–biological interactions had been systematically inspected at the soil particle level (J. J. Gao et al., 2020). However, the effects of physical and chemical stabilization on different soil carbon pools are not fully understood and quantitative data are scarce.

Dissolved organic matter (DOM) plays important roles in connecting various ecological compartments (Zsolnay, 2003). DOM is the energy source of heterotrophic organisms, and the source and carrier of nutrients, organic pollutants, and heavy metals in the soil and water environment (Qualls & Haines, 1991, Haitzer et al., 1998, Judd et al., 2006, Bolan, et al., 2011). The chemical characteristics of

irrigation water showed significant impacts on the DOM migration in forest soils (Kalbitz et al., 2000; Münch et al., 2002), for example, Ca^{2+} ions in irrigation water were found to improve the DOM adsorption by soil clay minerals (W. B. Chen et al., 2013; Y. Gao et al., 2015; Kaiser, 1998) but when the Na^{+} content in water is high enough, Na^{+} can replace Ca^{2+} in bridge bonds with DOM and, therefore, increases the DOM leaching in soils (Gu et al., 2019; Reemtsma et al., 1999). The chemical composition of DOM has important influences on the evolution and fractionation of DOM in soil (Scott & Rothstein, 2014; Stutter et al., 2006), DOM enriched with high apparent molecular weight components or/and aromatic carboxyl structures strongly interacts with soil minerals (Oren & Chefetz, 2012). The migration of DOM in karst areas and its control processes are little known, most of the previous work has been around the formation and recording information of speleothem (Lechleitner et al., 2017). Lechleitner et al. (2017) studied the changes in the composition of DOM in the waters between soil and cave systems in a karst area and found that mineral adsorption and microbial reworking are the reasons for the observed trends in DOM composition. Studies also showed that the migration of DOM with groundwater is very important for many karst processes, and DOM is an important source of nutrients for karst fauna (Shabarova et al., 2014). However, the influence of karst water with different chemical characteristics on the leaching of DOM in karst soils has not been reported yet.

Limestone soil is the representative soil of karst areas, and is widely developed in the karst area of southwest China (Wang et al., 2004). Limestone soil is believed to have originated mainly from the weathering of carbonate rocks (Bai et al., 2020; Cao et al., 2004). Compared with zonal soils such as yellow soil and red soil in the karst area of southwest China, limestone soils have relatively higher soil organic matter (SOM) content, and the humification degree of SOM of limestone soil is usually higher (Cao et al., 2003). Limestone soils with high SOM content usually have high Ca^{2+} content (Q. Chen et al., 2020; Di et al., 2019; He et al., 2019; Zhang et al., 2020), since Ca^{2+} can combine with SOM to form stable calcium humate, thereby improving the stability of SOM in limestone soil (H. M. Tang et al., 2021; Tipping et al., 1995), in return for SOM accumulation, more Ca^{2+} can be retained in the limestone soil without being leached. The Ca^{2+} bridges between SOM and soil minerals help to form soil aggregates, thereby physically protecting SOM from erosion and biodegradation (Kerr & Eimers, 2012; Kretzschmar & Sticher, 1997; Tipping & Hurley, 1992). However, the mechanism of the occurrence and evolution of SOM in limestone soil has not yet been elucidated, and there are very few relevant research reports.

Runoff water controls the erosion and redistribution of soils as well as the migration of SOM (Lal, 2005). Water in karst areas, including rainwater, surface runoff, and groundwater, usually contains high Ca^{2+}. For example, the concentrations of Ca^{2+} in groundwater, surfacewater, and rainwater of the karst area of southwest China are 1.10–5.39, 0.15–0.90, and 0.04–0.14 mmol L^{-1}, respectively, which are higher than corresponding values in non-karst areas (Cao et al., 2003; G. L. Han et al., 2008; Liu et al., 2006; Zhou et al., 2017). However, under leaching of Ca-rich water, the migration and fractionation of DOM in limestone soil is little known.

The soil column leaching experiment is recommended to conduct soil column leaching experiment in simulating natural scenes like irrigation (Setia et al., 2013; Tavakkoli et al., 2015) and helpful to collect the experimental information of different layers of soil (Rashad et al., 2010). The soil column leaching studies were conducted on agricultural soils (Gu et al., 2019) and forest soils (Münch et al., 2002) to investigate the leaching behavior of DOM by irrigation water of different chemical characteristics; however, the dynamic leaching behavior of DOM in limestone soil profiles of karst area is rarely reported and poorly understood, which has hindered the accurate estimation of the carbon sequestration potential of limestone soil in karst areas.

In this study, we assume that the Ca^{2+} content of karst water would affect the chemical properties and migration of DOM in limestone soil during erosion and irrigation. To test our hypothesis, four limestone soil samples were collected from the surface and the subsurface layers of two limestone soil profiles in the karst area of southwest China for soil column leaching experiments. The dynamic leaching process of DOM in these limestone soils by the simulated karst water of different Ca^{2+} concentrations is systematically studied, and a variety of instrument techniques are used to monitor the real-time quantity and quality changes of DOM during the leaching. The purpose of this study is to explore the potential mechanism of DOM fractionation and migration in limestone soils when leached by karst water of different Ca^{2+} concentrations.

2 | MATERIALS AND METHODS

2.1 | Limestone soil sample

Two surface soils (H1 and S1, 0–15 cm) and two sub-surface soils (H2 and S2, 15–40 cm) were collected from two limestone soil profiles, namely HT (26°22′N, 105°46′E) and SJ (26°14′N, 105°46′E), respectively. These two limestone soil profiles are located near the Puding Karst Ecosystem Observation and Research Station, Puding, Guizhou, China. They were selected because they are located on the top of carbonate rock hills and far away from villages; therefore, the soil samples are native limestone soils and suffer less influence from human activities. The vegetation cover of HT is a mixed forest, and the vegetation cover of SJ is weeds. The limestone soil sample was air-dried in a dark, ventilated room, slightly crushed through a 10-mesh sieve, and then stored in brown glass jars after picking out visible stones and vegetation residues. The limestone soils from the surface layer (H1, and S1) showed a blackish colour (Munsell code: 10B/1/2), while limestone soils from the subsurface layer showed brown (H2) and reddish (S2) colors.

Detailed properties of the four limestone soil samples, including soil texture, organic carbon content, pH, cation exchange capacity (CEC), and exchangeable calcium percentage (ECP), are summarized in Table 1.

2.2 | Column experiment

The soil column leaching experiment is illustrated in Figure 1. The column is an acrylic glass column of 5 cm in diameter and 25 cm in length, the inner face of the column was roughened previously to avoid preferential flow along the wall (Xiao & Xiao, 2021). An exact amount of limestone soil sample (220.0 g, dry weight) was gently packed in the column with a layer of acid-washed quartz sand (20-mesh) and two fibreglass filters (2.4 and 0.45 μm, Fiberglass Membranes, Jinjing, China) were placed at both top and bottom of the column. The preliminary experiments show that the soil columns of different limestone soils have a similar pore volume of 140 ± 2 ml. The purpose of the quartz sand and fiberglass filters is to unify the flow and to keep fine soil particles. The 2.4 μm filter is used for the primary filtration, and the 0.45 μm filter is used for the secondary filtration.

The leaching fluid was prepared by $CaCl_2$ (analytical degree, Fisher Scientific, USA) and deionized water (DI-water). The DI-water was used as a leaching fluid for blank and comparison purposes; the 0.05, 0.50, and 2.50 mmol L^{-1} of Ca^{2+} were used to simulate rainwater, surface runoff, and groundwater in the karst area of southwest China (Cao et al., 2003; G. L. Han et al., 2008; Liu et al., 2006; Zhou et al., 2017). All leaching experiments were conducted at 24 ± 1°C in a temperature-controlled chamber. Before leaching, the soil column was filled with a leaching fluid from bottom to top using a peristaltic pump and then kept upright overnight to ensure saturation as much as possible. Then, the soil column was continuously fed with the same leaching fluid by the peristaltic pump from top to bottom at a flow rate of 2 ml min^{-1}. The leachate (5 ml) was collected every 20 min, and a total of 24 leachate samples were collected for every soil column leaching experiment. The detailed experiment conditions are list in Table 2.

2.3 | Analytical methods

2.3.1 | Characterization of soils and leachates

The pH of limestone soil was measured in DI-water with a soil–water ratio of 1:5. The particle size distribution of soil was measured by a laser particle diameter analyzer (Mastersizer 2000, Malvern, UK). The total organic carbon (TOC) of limestone soil was determined by an elemental analyzer (Vario El III, Elementar, Germany) after removal of carbonate by overdosed HCl. The CEC of limestone soil was

TABLE 1 Physical and chemical properties of limestone soils

	Depth	Clay	Silt	Sand	pH	TOC	DOC	CEC	ECP
	cm	%				($g \cdot kg^{-1}$)	($g \cdot kg^{-1}$)	($cmol \cdot kg^{-1}$)	%
H1	0–15	14.8	56.1	29.1	7.61	87.54	1.64	75.42	75.1
H2	15–40	11.7	45.5	42.8	7.76	53.06	0.51	31.27	79.9
S1	0–15	16.9	57.9	25.2	7.81	48.95	0.99	39.46	54.5
S2	15–40	13.9	44.1	42.0	7.94	13.42	0.31	31.05	48.8

Abbreviations: CEC, cation exchange capacity; DOC, soil dissolved organic carbon content; ECP, exchangeable calcium percentage; TOC, total organic carbon content of soil

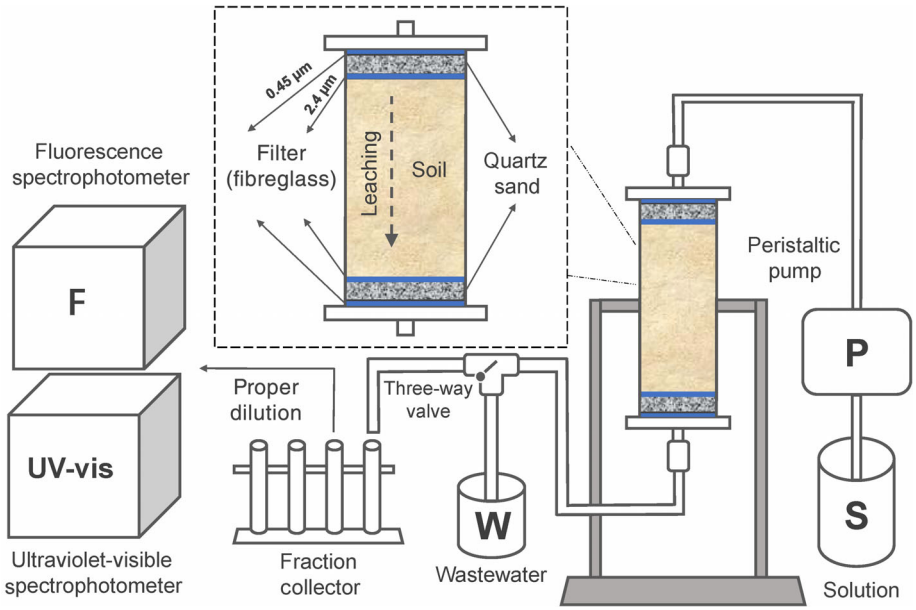

FIGURE 1 Schematic diagram of soil column leaching experiment [Colour figure can be viewed at wileyonlinelibrary.com]

TABLE 2 Soil column leaching experiment scheme and details

Soil	Mass (g)	Temperature (°C)	Pore volume[a] (ml)	Eluent	Ca^{2+} concentration ($mmol \cdot L^{-1}$)	Pumping rate[b] ($ml \cdot min^{-1}$)
H1	220	24 ± 1	141	DI-water	0	2 ± 0.05
H2			142	$CaCl_2$	0.05	
S1			138		0.5	
S2			139		2.5	

[a]Because of the different soil densities and porosities, there were some differences between the soil columns in pore volume
[b]The internal pressure of the soil column would lead to an unstable flow rate at the beginning of the experiment. The flow rate would stabilize at 2 $ml \cdot min^{-1}$ when the experiment was carried out for 20 min

calculated using the ammonium acetate method (Sumner & Miller, 1996), and the ECP was calculated following the method described elsewhere (Kim et al., 2018). The DOC concentration in eluents was determined by an elemental analyzer (Vario TOC cube, Elementar, Germany) following the method described by Bolan et al. (1996).

2.3.2 | Spectral analyses

The UV–Vis absorbance spectrum of leachate over the wavelength range of 200–800 nm was measured by a UV–Vis spectrophotometer equipped with a 10-mm quartz cuvette (Cary 300, Agilent) at a scanning rate of 300 nm min^{-1}. Parameters $SUVA_{254}$ and S_R were used to describe the molecular characteristics of DOM in leachate. $SUVA_{254}$ is the UV absorbance at 254 nm normalized by the organic carbon content, which positively correlates to the aromaticity of DOM (Weishaar et al., 2003). S_R is the ratio of spectral slopes in 275–295 nm and 350–400 nm, which negatively correlated to the apparent molecular weight of DOM (Helms et al., 2007). Their specific expressions are as follows:

$$SUVA_{254} = \frac{Abs_{254}}{DOC}, \tag{1}$$

$$a_\lambda = 2.303 \cdot Abs_\lambda / L, \tag{2}$$

$$S_{\lambda_0-\lambda} = \frac{\ln(a_{\lambda_0}) - \ln(a_\lambda)}{\lambda - \lambda_0}, \tag{3}$$

$$S_R = \frac{S_{275-295}}{S_{350-400}} \tag{4}$$

Where: Abs_{254} is the UV absorbance at 254 nm, a_λ is the absorption coefficient at λ nm, L is the path length of the quartz cuvette, λ_0 is the reference wavelength, and $S_{275-295}$ and $S_{350-400}$ are the spectral slopes in the range of 275–295 and 350–400 nm, respectively.

The 3D excitation-emission matrix (3D-EEM) fluorescence spectra of leachate were scanned at the same excitation/emission wavelengths (Ex/Em) of 200–600 nm with a same scanning rate of 2400 nm min^{-1} by a fluorescence spectrophotometer (F-4500, Hitachi, Japan). In order to avoid inner-filter effects, the leachate was diluted till its absorbance at 254 nm less than 0.3 (van de Weert, 2010). The Raman effects were removed by subtracting the spectrum of DI-water from the spectrum of the leachate. The parallel factor analysis (PARAFAC) was applied on 3D-EEM fluorescence spectra of leachates to identify the potential individual fluorescent components (Stedmon & Bro, 2008). PARAFAC decomposes the EEM spectrum into a set of trilinear and a residual array:

$$X_{ijk} = \sum_{f=1}^{F} a_{if} b_{jf} c_{kf} + \varepsilon_{ijk} \quad i = 1,\ldots,I;\ j = 1,\ldots,J;\ k = 1,\ldots,K, \tag{5}$$

Where: x_{ijk} is the intensity of fluorescence for the ith sample at emission wavelength j and excitation wavelength k. a_{if} is directly proportional to the concentration of the fth analyte in the ith sample. b_{jf} and c_{kf} are the model parameters representing emission and excitation spectra of the underlying fluorophores, respectively. F is the column number of the loading matrix, representing the number of components in the model. ε_{ijk} is the residual.

PARAFAC analyses were conducted by MATLAB R2016a (MathWorks, USA). All EEMs of leachates could be fit well by models of 3–6-components. The core consistency, the sum of the squared errors (SSE), and split-half validation were adopted to evaluate fitting results and to determine the most suitable number of components (Singh et al., 2010; Stedmon & Bro, 2008). The results of PARAFAC are provided in the attached Table S1 and Figures S6–S9.

F_{MAX} is the parameter representing the fluorescence intensity. F_{MAX} is proportionate to the quantity of the component and helps identify the composition relationship of different components, that is, the percentage of the component (%C) (Pifer et al., 2011). The %C reflects the share of the component in the EEM (Dainard et al., 2015; Kowalczuk et al., 2009). The definition of %C is as follow:

$$\%Ci = \frac{F_{MAX\ i}}{\sum F_{MAX\ 1} + F_{MAX\ 2} + \cdots + F_{MAX\ I}} \quad i = 1,2,\ldots,I, \tag{6}$$

Where: %Ci is the percentage of component i in the EEM. $F_{MAX\ i}$ is the maximum fluorescence intensity of component i.

2.3.3 | Kinetic equation fitting

Several kinetic equations (e.g., Elovich equation, double constant equation, first-order equation, and second-order equation) were employed to fit the variation of DOC loss with the leaching time and were compared according to the least-square regression analysis. Results indicated that the Elovich equation is the best fitting model for this study. The Elovich equation was widely used for modeling the chemisorption kinetics and can give reaction rate and activation energy of sorption kinetic processes (Atkinson et al., 1970; Elkhatib & Hern, 1988; Inyang et al., 2016). The expression of the Elovich equation is as follows:

$$D = \frac{1}{\beta}[\ln(k\beta) + \ln(t)], \quad (7)$$

Where: D is the DOC loss (mg) from soil, k is the apparent reaction rate constant (mg·min^{-1}), β is the constant associated with the desorption activation energy, and t is the leaching time (min).

3 | RESULTS

3.1 | Variation of DOC in leachates

The variations of the DOC concentration in leachates are presented in Figure 2. In general, the DOC concentration of leachates showed a two-stage variation, it decreased rapidly in the early period, after the volume of leachate reached approximately 450–500 ml, it became either slightly decreasing or relatively stable and kept until the end of experiment. The influence of the Ca^{2+} concentration on the DOC concentration of leachates was significant only in the first stage, the higher was the Ca^{2+} concentration of eluent the low was the DOC concentration of leachate. The DOC concentration of leachate correlated positively with the TOC of corresponding soils. Briefly, the initial and ending DOC concentrations of leachate from H1 soil columns were 875.2–1047.4 mg L^{-1} and 35.1–50.4 mg L^{-1}, respectively, all of which are the highest compared with those of other soils, and which consists H1 has the highest TOC of 87.5 g·kg^{-1}; the initial and ending DOC concentrations of leachate from H2 soil column were 311.4–386.3 mg L^{-1} and 10.0–19.8 mg L^{-1}, respectively, all of which are lower than those of the H1 soil, consistent with that the H2 soil had a

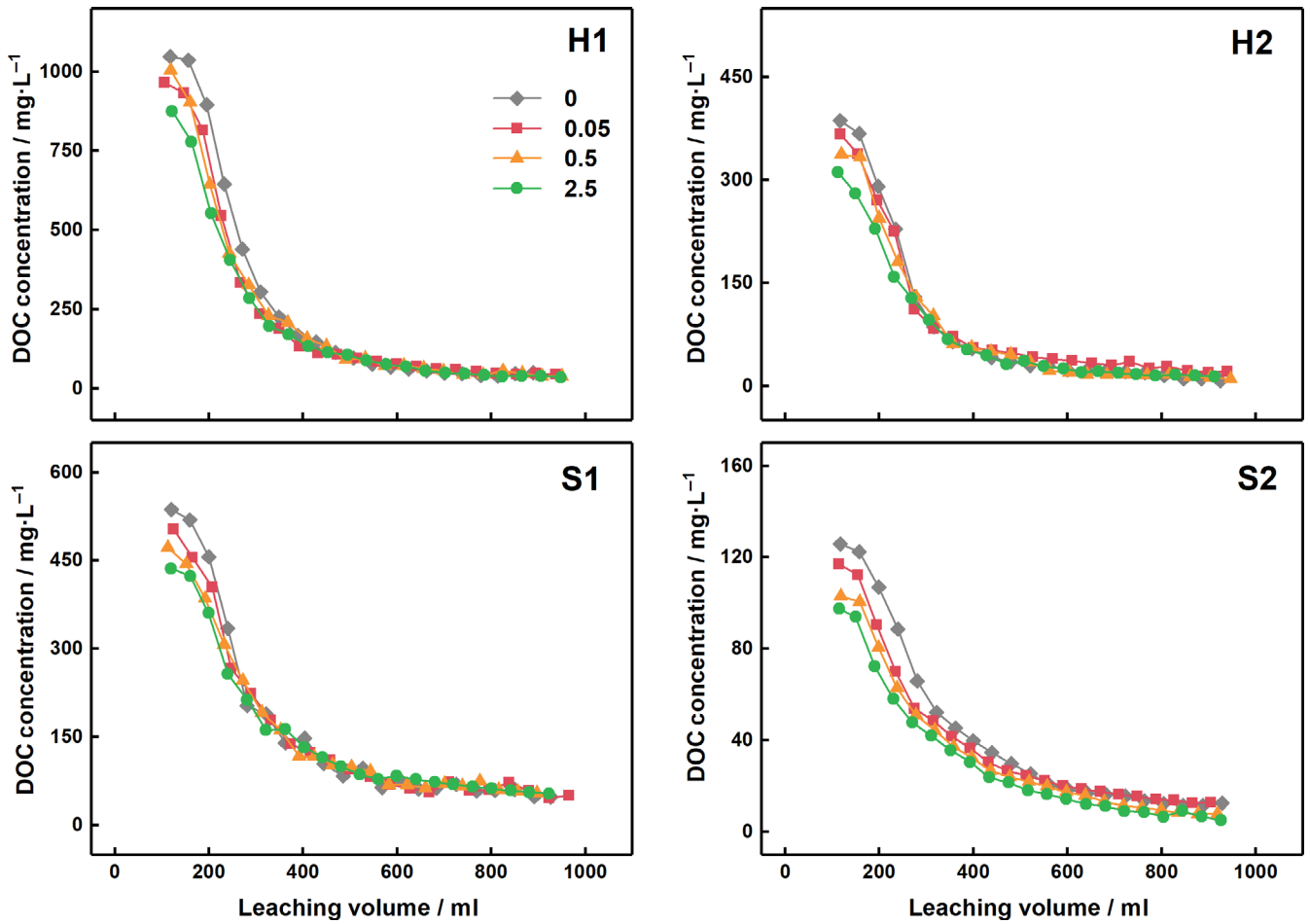

FIGURE 2 Temporal variation of DOC concentrations in leachates. H1, H2, S1, and S2 are four limestone soils, and 0, 0.05, 0.5, and 2.5 are Ca^{2+} concentrations (mmol L^{-1}) of eluents [Colour figure can be viewed at wileyonlinelibrary.com]

relatively lower TOC of 53.1 g kg^{-1}; the TOC of S1 was 49.0 g kg^{-1}, the initial and ending DOC concentrations of leachate from S1 soil columns were 436.5–536.6 mg L^{-1} and 48.3–54.7 mg L^{-1}, respectively; the S2 soil had the lowest TOC of 13.4 g kg^{-1}, the initial and ending DOC concentrations of leachate from S2 soil columns were also the lowest, 97.4–125.8 mg L^{-1} and 5.1–12.8 mg·L^{-1}, respectively. The accumulated DOC loss from soil columns of H1, H2, S1, and S2 was 212.2–239.2, 81.5–85.5, 149.8–159.0, and 31.8–35.8 mg, respectively, which also shows the positive correlation with their TOC contents.

3.2 | Spectroscopic characteristics of leachates

3.2.1 | UV–Vis spectra

The changes of $SUVA_{254}$ and S_R of leachate are shown in Figure 3. $SUVA_{254}$ of leachate appeared an upward trend for all experiments, indicating that the proportion of aromatic components in leachates increased as the leaching experiment progressed. $SUVA_{254}$ of leachate was notably correlated with the Ca^{2+} concentration of eluent, the higher is the Ca^{2+} concentration, the lower is the numerical value of $SUVA_{254}$. Nevertheless, the effect of Ca^{2+} concentration on $SUVA_{254}$ was much larger for surface soils (H1 and S1) than for subsurface soils (H2 and S2). The variation of S_R of leachate showed an opposite trend. The value of S_R decreased as the leaching experiment proceeded, indicating the apparent molecular weight of DOM in leachates increased. S_R of leachate was also affected by the Ca^{2+} concentration of eluent; the higher the Ca^{2+} concentration, the lower is the value of S_R of leachate. In summary, the trends of $SUVA_{254}$ and S_R variations indicated that DOM of smaller apparent molecular weight and aromaticity was leached from soil columns earlier, while DOM of larger apparent molecular weight and aromaticity was leached later.

3.2.2 | Results of EEM-PARAFAC

The 3D-EEM fluorescence spectra of all leachates are shown in the supporting information (Figure S1–S4). The model analysis gave the loading information and suggested that the four-component model adequately resolved the leaching DOM for all leaching experiments (Figures S6–S9). The Ex/Em loadings of leachate DOM were matched by the OpenFluor database (openfluor.lablicate.com) under a constraint of 95% similarity. Although the Ex/Em spectra of components

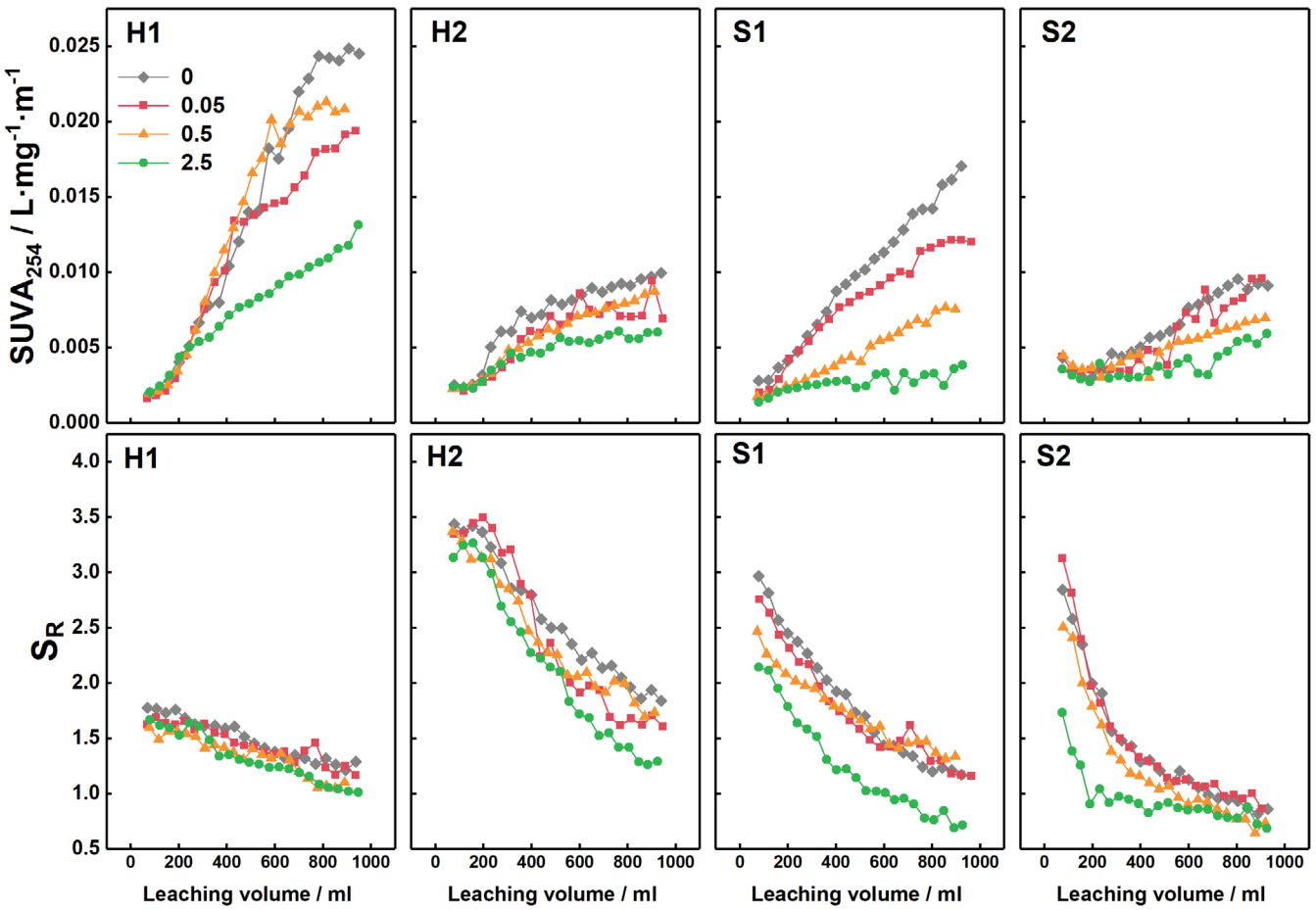

FIGURE 3 Temporal variations of $SUVA_{254}$ and S_R of leachates. H1, H2, S1, and S2 are four limestone soils, and 0, 0.05, 0.5, and 2.5 are Ca^{2+} concentrations (mmol·L^{-1}) of eluents [Colour figure can be viewed at wileyonlinelibrary.com]

obtained for different limestone soils were not identical, components of similar Ex/Em spectra were classified into one type, which was defined and interpreted by previous studies (P. Coble, 2007; Henderson et al., 2009). For example, the maximum Ex/Em wavelengths of a component in H1 were 280/330 nm, which were close to those (280/340 nm) for a component in H2: these two components were interpreted as the same component 3 (C3), classified as the tryptophan-like compounds. The specific maximum Ex/Em wavelengths are listed in the attached Table S1.

The information of all components resolved by this study is shown in Table 3. Component 1 (C1) was signed as the UVC humic-like DOM, representing the terrigenous organic matters including humic and fulvic acids (P. G. Coble, 1996); component 2 (C2) and component 3 (C3) were the tyrosine-like and tryptophan-like compounds, representing organic matters such as amino acids and fluorescent proteins (P. Coble et al., 1998); component 4 (C4) was the marine humic-like compounds, which may come from human activities such as agriculture and domestic wastewater (Stedmon & Markager, 2005); component 5 (C5) represented the UVA humic-like compounds, which may derive from terrigenous or agricultural DOM (P. Coble, 2007, Henderson et al., 2009). We found that four components for each of the four limestone soils employed in this study and limestone soils from the same soil profile had the same components, for example, C1, C3, C4, and C5 for H1 and H2, C2, C3, C4, and C5 for S1 and S2, respectively.

The contribution of different components (%C) was calculated by Equation 6, and the results are listed in Figure 4. It can be seen that contributions of different components changed differently along the process of leaching, but the certain trend for any component in a leaching experiment kept constant. For example, %C1 increased constantly and %C3 decreased constantly in experiments of H1 and H2 soil columns. The contributions of different components in different soil leaching experiments changed differently. For example, %C2 decreased in S1 soil leaching experiments but increased in S2 soil leaching experiments. The different change trends for a certain component in different soil experiments indicated that chemistry of component was not the only factor controlling its leaching behaviors, soil texture and complicated interactions between components and soil minerals might also play important roles.

As shown in Figure 4, the Ca^{2+} concentration had visible but inconsistent influence on the leaching behaviors of components. However, influences of the Ca^{2+} concentration were not consistent among different components, for example, when the Ca^{2+} concentration of eluent was the highest (2.5 mmol L^{-1}), corresponding %C2 and %C3 were highest, but corresponding %C4 and %C5 were the lowest. These results might suggest that when limestone soils suffer hydrodynamic erosions, the higher Ca^{2+} concentration runoff may be propitious to the leaching of C3 and C2 but inhibit the leaching of C4 and C5.

4 | DISCUSSION

4.1 | Dynamic characteristics of DOC release

The dynamic DOC release process of this study is consistent with previous reports (Gu et al., 2019; Y. S. Han & Tokunaga, 2014). Figure 2 showed that DOC of leachates were relatively high at the beginning, decreased quickly in the early leaching stage, and then became relatively stable or slightly decreasing in the later leaching stage. These two leaching stages reflect the binding conditions of SOM with the soil matrix, the rapid declining stage of the leachate DOC indicates that amount of dissociation of SOM from the soil matrix is limited, while the stable leaching stage may be due to the limited rate of SOM exchange process (Reemtsma et al., 1999; Tiemeyer et al., 2017).

According to the soil DOC data in Table 1, the cumulative curves of the percentage of soil DOC loss under different leaching fluids are calculated and plotted in Figure 5. The cumulative curve of the percentage of DOC loss also had two stages, a rapid increasing stage and a relatively slow accumulation stage, which are inversely proportional to the DOC concentration curve in the leachate (Figure 2). The Ca^{2+} concentration of eluent showed consistent influence on the percentage of DOC loss in all soils, the higher is the Ca^{2+} concentration, the smaller is the percentage of DOC loss. When the Ca^{2+} concentration increased from 0 to 2.5 mmol L^{-1}, percentages of DOC loss in H1, H2, S1, and S2 soils decreased from 66.3% to 58.8%, from 76.2% to 72.4%, from 73.0% to 68.8% and from 52.5% to 46.6%, respectively, the limestone soils test in this study reduced by an average of 5.4%.

TABLE 3 Components resolved for leachate DOM and their interpretation

	This study		Previous studies				
Number	Ex max (nm)	Em max (nm)	Peak name	Ex max (nm)	Em max (nm)	Component	Description
C1	240–270	450–470	A	237–270	400–500	UVC humic-like	Fulvic and humic acid, allochthonous, terrestrial
C2	240–280	300–330	B	225–237 (280)	309–331 (300)	Tyrosine-like	Autochthonous
C3	280	330–350	T	225–237 (280)	330–410	Tryptophan-like	Autochthonous
C4	310	390–420	M	290–310	370–420	Marine humic-like	Anthropogenic from wastewater and agriculture
C5	280, 340–380	460–500	C	300–380 (280)	400–500	UVA humic-like	Anthropogenic, agriculture, terrestrial

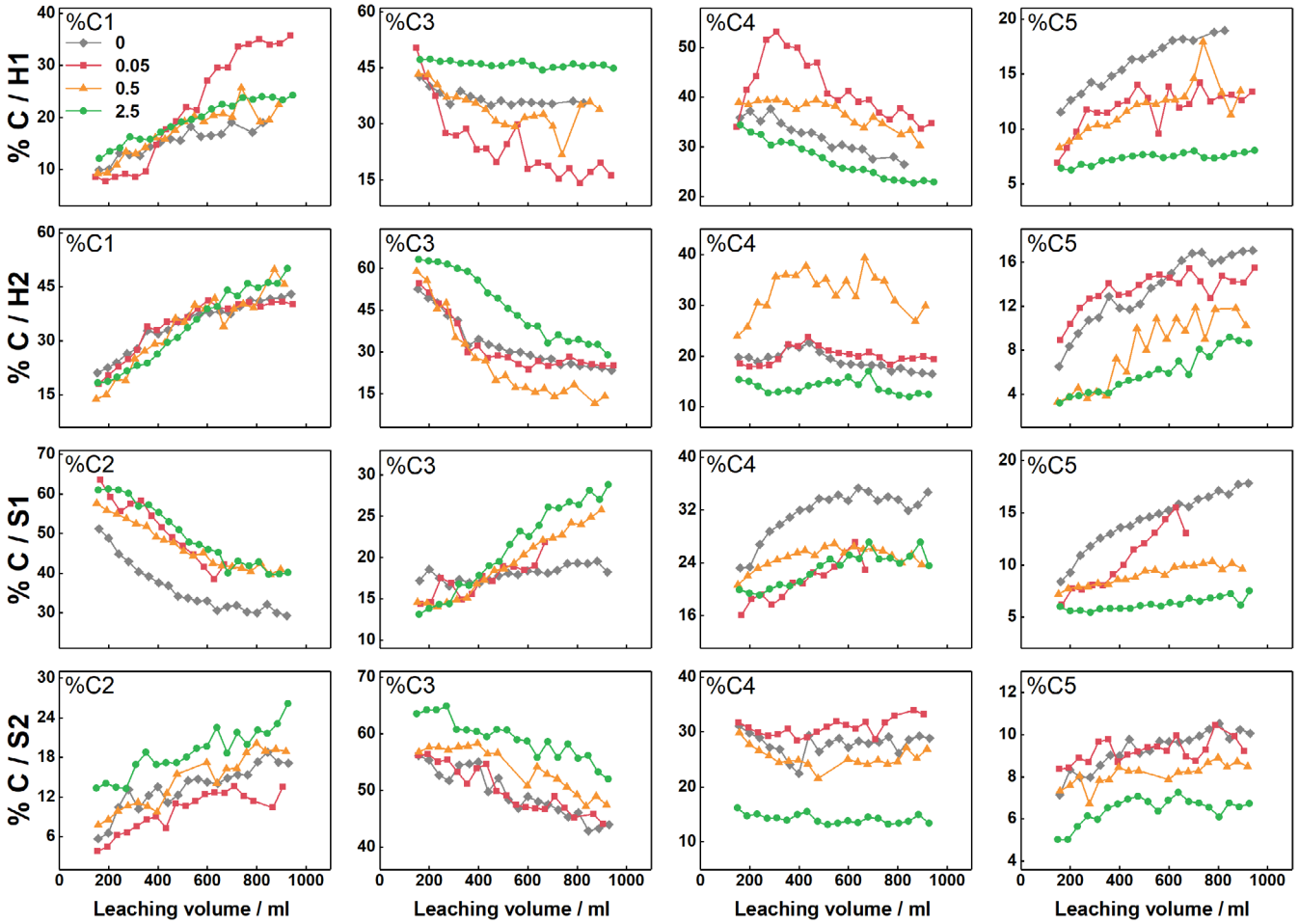

FIGURE 4 Contributions of components (%C) in leachates from different soils. H1, H2, S1, and S2 are four limestone soils, and 0, 0.05, 0.5, and 2.5 are Ca^{2+} concentrations (mmol·L^{-1}) of eluent [Colour figure can be viewed at wileyonlinelibrary.com]

This result supports the view that Ca^{2+} protects SOM from rapid erosion and degradation in the soil (Kerr & Eimers, 2012), and further shows that the protective effect of Ca^{2+} increases with the increase of Ca^{2+} concentration.

The fitting results of the Elovich equation are shown in Table 4 and Figure S10. With the increase of the eluent Ca^{2+} concentration, the rate constant k showed a downward trend, indicating that with the increase of the eluent Ca^{2+} concentration, the desorption rate of DOC in the soil matrix decreased. The reaction activation energy constant β showed an upward trend with the increase of the eluent Ca^{2+} concentration, indicating when the eluent Ca^{2+} concentration increased, the activation energy for DOC desorption in the soil matrix increased.

4.2 | Effects of soil properties on DOC release

The leaching behaviour of DOC in different limestone soils was different. After continuous leaching by four eluents for 8 h, the leached amounts of DOC from H1, H2, S1, and S2 soils were from 239.2 to 212.2 mg, from 85.5 to 81.2 mg, from 159.0 to 149.8 mg, and from 35.8 to 31.8 mg, respectively. The percentages of DOC loss of H1, H2, S1, and S2 soils were from 66.3% to 58.8%, from 76.2% to 72.4%, from 73.0% to 68.8%, and from 52.5% to 46.6%, respectively. These data indicated that the amount of DOC leached from the soil column was positively correlated with DOC and TOC of the corresponding soil (Table 1). The spectra characteristics of leachates also differed from soil to soil under the same eluent, indicating that the nature of the soil determined the chemical properties of the leached DOC. The increase in $SUVA_{254}$ of surface soils (H1 and S1) was much greater than of subsurface soils (H2 and S2), while the S_R values of H1 had decreased slightly but the S_R values of other soils decreased significantly (Figure 2). In addition, EEM-PARAFAC analysis showed that component 2 (C2), tyrosine-like compounds, could be distinguished in soils from the SJ profile, but could not be distinguished in soils from the HT profile (Figure 4). In summary, the leaching amount of DOC in the four target limestone soils was complicatedly affected by the quantity and quality of SOM and the nature of soil matrix, and was closely related to the source of SOM and the stage of soil evolution.

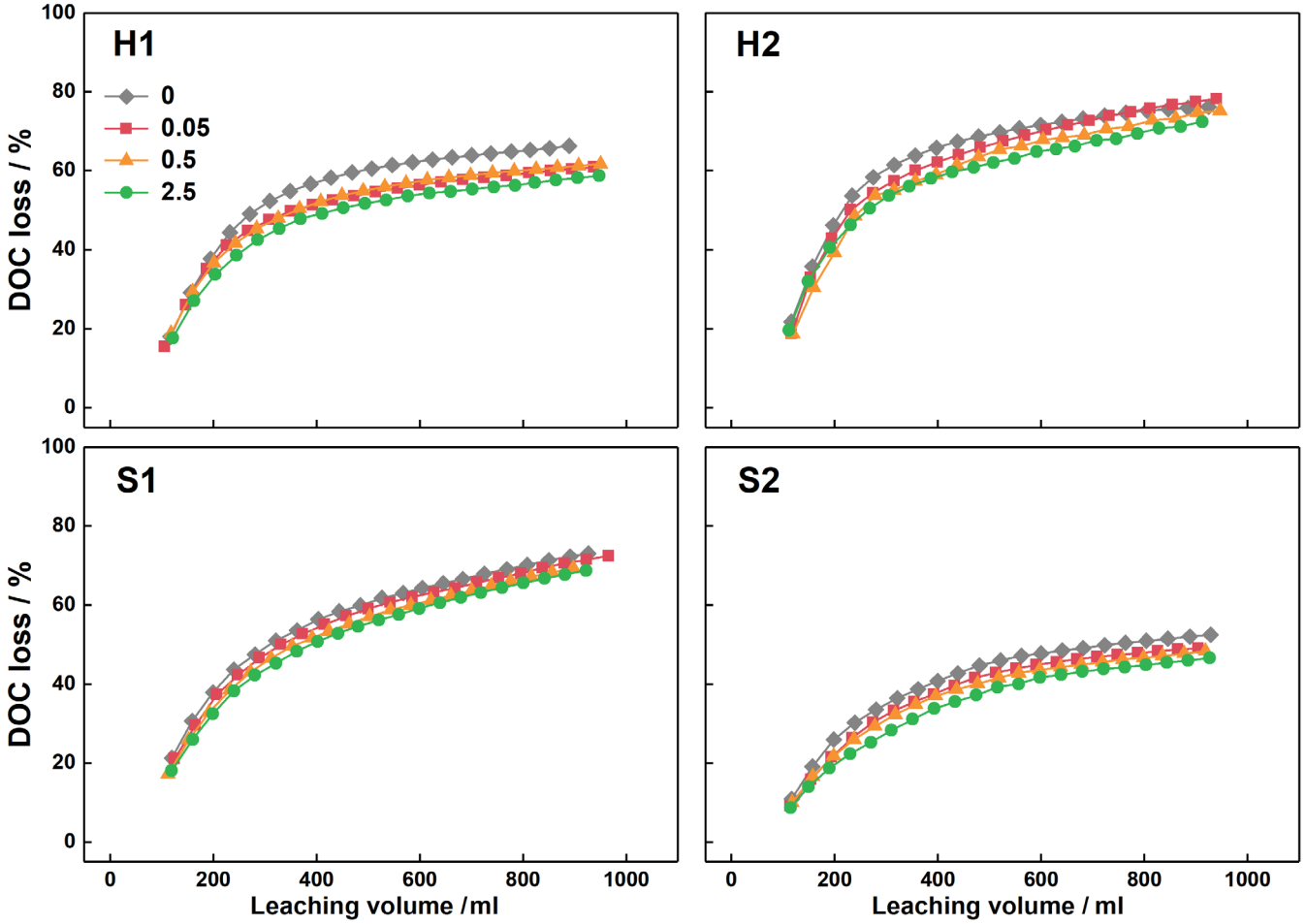

FIGURE 5 Variations of the percentage of DOC loss in different soils with leaching. 0, 0.05, 0.5, and 2.5 are the Ca^{2+} concentrations ($mmol \cdot L^{-1}$) of eluent [Colour figure can be viewed at wileyonlinelibrary.com]

4.3 | Ca^{2+} effects on DOM leaching process

The influence of Ca^{2+} in the eluent on the leaching of DOC in limestone soil was reflected in the amount and the chemical characteristics of leached DOC. As shown in Figure 2, when the eluent Ca^{2+} concentration increased, the DOC content in leachate decreased accordingly, this was particularly obvious in the early stage of the leaching experiment but it was almost invisible in the late stage. We think this observation is very importance because it may indicate that the easily leaching DOC of limestone soils is more affected by Ca^{2+}, while the leaching resistant DOC of limestone soils less affected by Ca^{2+}. When the eluent Ca^{2+} concentration increased, the percentage of DOC loss for all limestone soils showed a downward trend. For example, compared with DI-water, when the limestone soil was leached by 0.05, 0.50, and 2.50 $mmol \cdot L^{-1}$ Ca^{2+} eluents, the percentage of DOC loss reduced by 0.6%–7.5% (Figure 5).

The concentration of Ca^{2+} also affected the chemical characteristics of DOC in leachates. As mentioned earlier, different Ca^{2+} concentrations of eluent affected the molecular structure of leached DOM. This is consistent with previous observations (W. B. Chen et al., 2013; Y. Gao et al., 2015; Gu et al., 2019; Kaiser, 1998; Kerr & Eimers, 2012; Kretzschmar & Sticher, 1997). Our results further indicated that high concentration of Ca^{2+} will exacerbate this phenomenon. For comparison, the changes of $SUVA_{254}$ and S_R were plotted for different Ca^{2+} concentrations of eluent in Figure 6. Similarly, the changes of %C in the leachate are plotted in Figure 7. It can be clearly seen from Figure 6 that as the Ca^{2+} concentration in the eluent increases, $SUVA_{254}$ and S_R of all leachates have a decreasing trend, indicating the aromaticity of leached DOC decreased and the molecular weight of leached DOC increased. The results of S_R show that the DOM has a higher molecular weight in a high Ca^{2+} environment. The underlying mechanism may be the bridging and complexing ability of Ca^{2+}, that is, Ca^{2+} can act as the ionic bridge to connect negatively charged SOM with soil minerals and other SOMs to form aggregates of high apparent molecular weight (Schaumann, 1999). The results of $SUVA_{254}$ may reflect that Ca^{2+} can connect aromatic SOMs with soil minerals or/and the increased hydrophobicity of aromatic SOMs in high-Ca^{2+} eluents, all of which may lead to a decrease in the aromaticity of DOM in the leachate.

With the increase of the eluent Ca^{2+} concentration, the %C exhibited complex changes, as shown in Figure 7. The most obvious trend is that %C5 decreases as the eluent Ca^{2+} concentration

TABLE 4 The Elovich equation fitting results for the DOC loss in leaching experiments

Sample	Ca^{2+} concentration mmol·L^{-1}	k^a Mg·min^{-1}	β^b 10^{-3}	R^2
H1	0	4.00 ± 0.27	12.05 ± 0.56	0.96
	0.05	3.60 ± 0.24	13.13 ± 0.60	0.96
	0.5	3.90 ± 0.25	13.34 ± 0.56	0.96
	2.5	3.61 ± 0.22	14.01 ± 0.56	0.97
H2	0	1.52 ± 0.11	34.44 ± 1.71	0.95
	0.05	1.36 ± 0.07	33.08 ± 1.19	0.97
	0.5	1.29 ± 0.07	34.35 ± 1.26	0.97
	2.5	1.30 ± 0.07	36.69 ± 1.31	0.97
S1	0	2.57 ± 0.09	19.35 ± 0.45	0.99
	0.05	2.51 ± 0.08	19.54 ± 0.43	0.99
	0.5	2.22 ± 0.08	19.88 ± 0.52	0.98
	2.5	2.22 ± 0.07	20.25 ± 0.47	0.98
S2	0	0.51 ± 0.02	77.35 ± 2.68	0.98
	0.05	0.45 ± 0.02	80.83 ± 2.87	0.97
	0.5	0.45 ± 0.02	83.38 ± 2.65	0.98
	2.5	0.41 ± 0.02	86.09 ± 2.97	0.97

[a]k is the apparent reaction rate constant
[b]β is the constant associated with the desorption activation energy

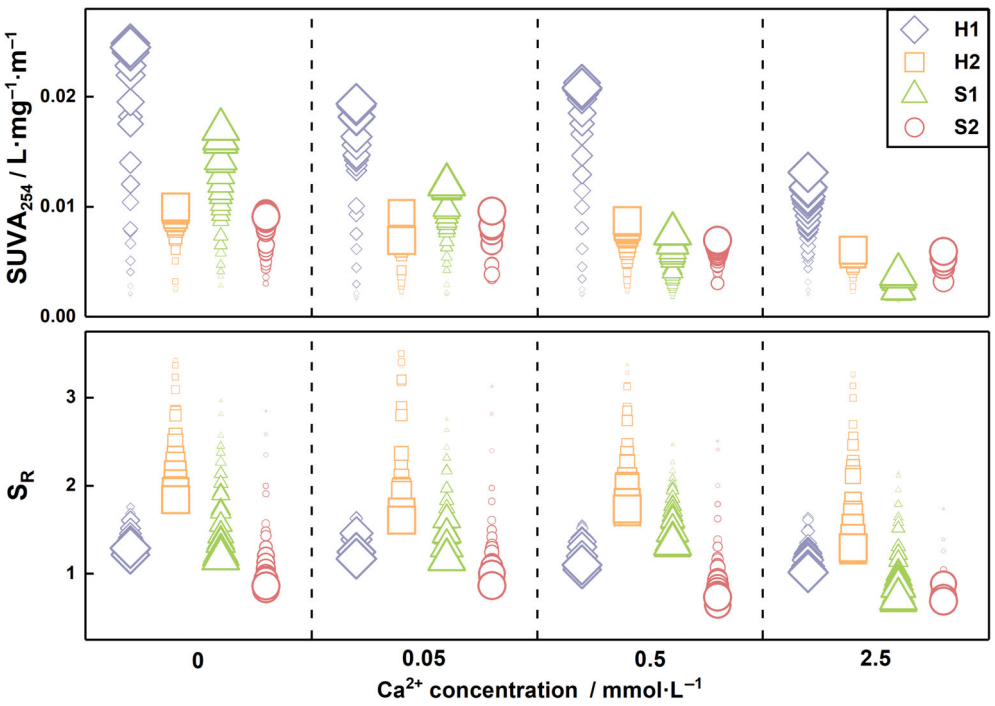

FIGURE 6 $SUVA_{254}$ and S_R of all leachates under different Ca^{2+} concentrations. Icons of the same shape and color represent the same limestone soil. The increase in icon size indicates the order of the leachate samples in the experiments [Colour figure can be viewed at wileyonlinelibrary.com]

increases. C5 is identified as a UVA humic-like compound in soil leachates, and is a kind of low molecular weight and aromatic SOM (Fellman et al., 2010; Gu et al., 2019; Ishii & Boyer, 2012). %C5 decreases with the increase of eluent Ca^{2+} concentration, which is consistent with the result of $SUVA_{254}$, that is, when the eluent Ca^{2+} concentration increases, $SUVA_{254}$ decreases. This means that the leaching of runoff with high Ca^{2+} concentration will enrich the aromatic SOM in the limestone soil. %C2 and %C3 show an overall upward trend with the increase of Ca^{2+} concentration, which may be due to the increased solubility of autochthonous amino acids after the reaction with Ca^{2+}. %C4 is the least as the eluent Ca^{2+} concentration is highest, but it fluctuates at other Ca^{2+} concentrations. C1 found in

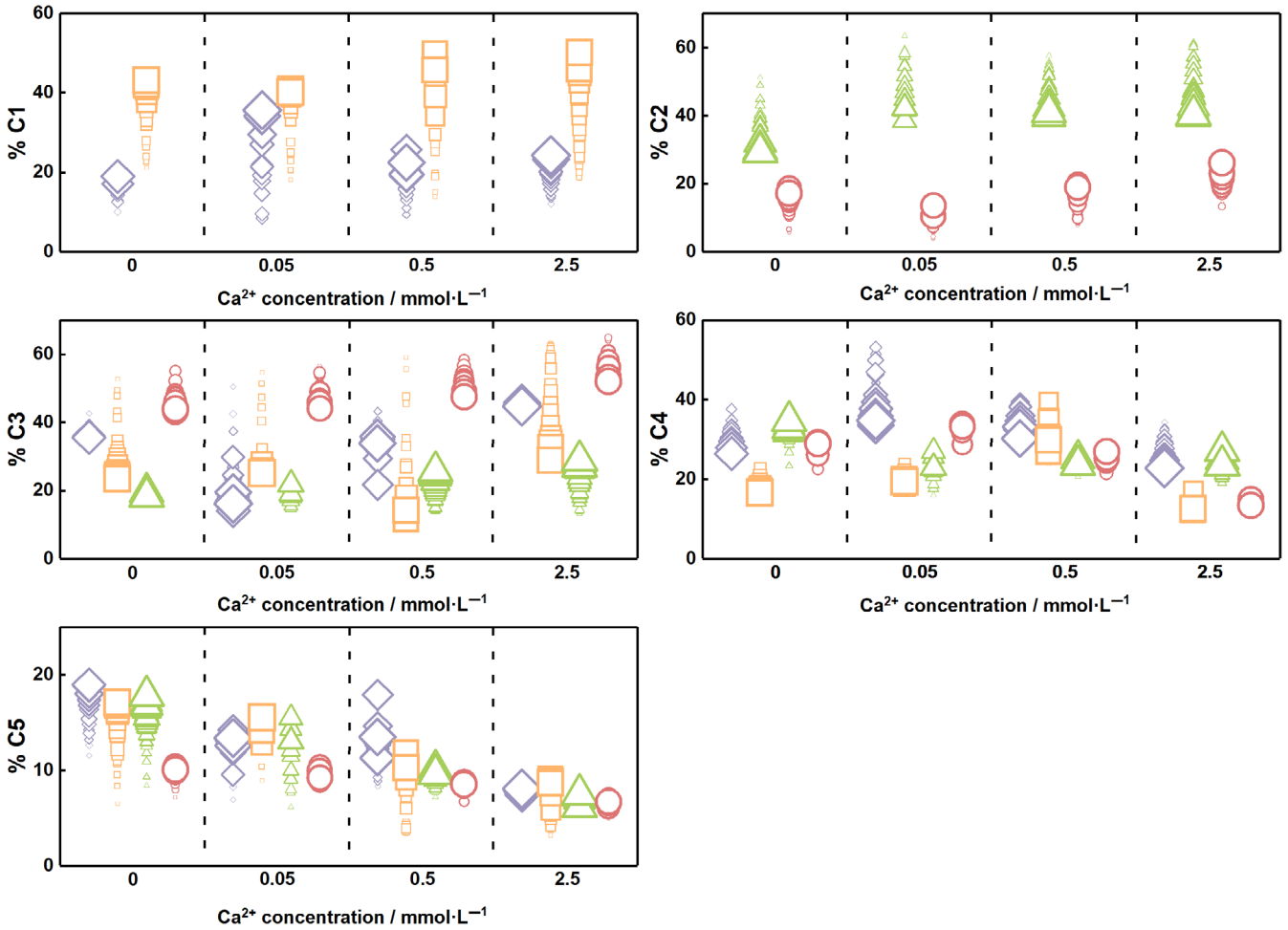

FIGURE 7 Change of %C under different Ca^{2+} concentrations. Icons of the same shape and color represent the same limestone soil; the increase in icon size indicates the order of the leachate samples in the experiments. Diamond: H1; square: H2; triangle: S1; and circle: S2 [Colour figure can be viewed at wileyonlinelibrary.com]

H1 and H2 soils is a UVC humic-like compound, representing high molecular weight SOM from various sources (Fellman et al., 2010, Gu et al., 2019, Ishii & Boyer, 2012). However, it should be noted that these spectral features of DOC are not quantitative but only have qualitative and statistical significance and should be interpreted with caution.

5 | CONCLUSIONS

In this study, the soil column experiment method was used to study the dynamic leaching processes of four kinds of limestone soil with four different Ca^{2+} concentration eluents, and the DOM in leachates with different leaching time was systematically characterized. The results show that the leaching process of DOM is in a two-stage mode, starting with the rapid DOM release and dilution stage and then the relatively stable DOM release stage. The leaching process can be well described by the Elovich equation. During the experiment, the aromaticity and apparent molecular weight of leached DOC continued to increase. The results also show that increasing the eluent Ca^{2+} concentration has a considerable influence on the leaching behavior of DOC. On-the-one-hand, the higher eluent Ca^{2+} concentration reduced the DOC content of leachate, and this effect is more significant in the early stage and becomes insignificant in the later stage of the leaching experiment. On-the-other-hand, the Ca^{2+} in the eluent has different effects on different chemical properties of DOC. For example, higher Ca^{2+} increases the apparent molecular weight of leached DOM and the leaching of amino acid-like compounds, and reduces the aromaticity of leached DOM and the leaching of humic-like compounds.

Consistent with the previous point of view, we believe that the complexation of Ca^{2+} with SOM and the bridging ability of Ca^{2+} between SOM and minerals are the reasons for the relatively poor efficiency of leaching DOC from limestone soils with high Ca^{2+} eluent. This study further shows that the stabilizing effect of Ca^{2+} is stronger on easily leached SOM than on relatively stable SOM. This may be a supplementary mechanism for the SOM stability in limestone soils of the karst area, and this mechanism is of great value for improving the understanding of soil carbon storage in karst areas. Nevertheless, we suggest that the soil in karst areas needs to be

further studied to verify this supplementary mechanism. This study reports for the first time the leaching behaviour of DOC in natural limestone soil profiles in the karst area under simulated karst water, and explores the potential mechanism that helps to understand the migration and fate of DOC in limestone soils, and provides theoretical support for increasing the soil carbon sink in karst areas.

ACKNOWLEDGMENTS

This study was supported by National Natural Science Foundation of China-Guizhou Joint Fund for Karst Science Research Center (U1612441), National Natural Science Foundation of China (41773147, 41273149). We gratefully acknowledge Dr. Xinyue Di and Dr. Haiming Tang for assistance in the experiment. We are grateful to the reviewers for their insightful comments that improved this manuscript greatly.

CONFLICT OF INTEREST

There is no conflict of interest in the results of this study.

DATA AVAILABILITY STATEMENT

All data generated or analysed during this study are included in this published article and its supplementary information files.

ORCID

Peiwen Xiao https://orcid.org/0000-0002-7519-4562
Baohua Xiao https://orcid.org/0000-0003-1329-6384

REFERENCES

Atkinson, R., Hingston, F., Posner, A., & Quirk, J. (1970). Elovich equation for the kinetics of isotopic exchange reactions at solid–liquid interfaces. *Nature*, *226*, 148–149. https://doi.org/10.1038/226148a0

Bai, Y. X., Zhou, Y. C., Zhou, X. W., & Zhang, C. L. (2020). Differentiating karst soil and soil in karst region: A case study of Houzhai River watershed in Puding County of Guizhou Province. *Soils*, *52*(2), 414–420. https://doi.org/10.13758/j.cnki.tr.2020.02.026

Batjes, N. (1996). Total carbon and nitrogen in the soils of the world. *European Journal of Soil Science*, *47*, 151–163. https://doi.org/10.1111/j.1365-2389.1996.tb01386.x

Bolan, N., Baskaran, S., & Thiagarajan, S. (1996). An evaluation of the methods of measurement of dissolved organic carbon in soils, manures, sludges, and stream water. *Communications in Soil Science and Plant Analysis*, *27*, 2723–2737. https://doi.org/10.1080/00103629609369735

Cao, J. H., Yuan, D. X., & Pan, G. X. (2003). Some soil features in karst ecosystem. *Advance in Earth Sciences*, *18*(1), 37–44. http://www.adearth.ac.cn/EN/10.11867/j.issn.1001-8166.2003.01.0037

Cao, J. H., Yuan, D. X., Zhang, C., & Jiang, Z. C. (2004). Karst ecosystem constrained by geological conditions in Southwest China. *Earth and Environment*, *32*(1), 1–8. https://kns.cnki.net/kcms/detail/detail.aspx?FileName=DZDQ200401001&DbName=CJFQ2004

Chen, Q., Shu, Y., Zhou, P., & Chen, Z. (2020). Calcium components of calcareous soil under different ecological restoration patterns in karst mountainous area. *Journal of Soil and Water Conservation*, *34*, 48–55. https://dx.doi.org/10.13870/j.cnki.stbcxb.2020.04.008

Chen, W. B., Smith, D. S., & Gueguen, C. (2013). Influence of water chemistry and dissolved organic matter (DOM) molecular size on copper and mercury binding determined by multiresponse fluorescence quenching. *Chemosphere*, *92*, 351–359. https://doi.org/10.1016/j.chemosphere.2012.12.075

Coble, P. (2007). Marine optical biogeochemistry: The chemistry of ocean color. *Chemical Reviews*, *107*, 402–418. https://doi.org/10.1021/cr050350+

Coble, P., Castillo, C., & Avril, B. (1998). Distribution and optical properties of CDOM in the Arabian Sea during the 1995 southwest monsoon. *Deep Sea Research Part II: Topical Studies in Oceanography*, *45*, 2195–2223. https://doi.org/10.1016/S0967-0645(98)00068-X

Coble, P. G. (1996). Characterization of marine and terrestrial DOM in seawater using excitation-emission matrix spectroscopy. *Marine Chemistry*, *51*, 325–346. https://doi.org/10.1016/0304-4203(95)00062-3

Dainard, P. G., Gueguen, C., McDonald, N., & Williams, W. J. (2015). Photobleaching of fluorescent dissolved organic matter in Beaufort Sea and North Atlantic subtropical gyre. *Marine Chemistry*, *177*, 630–637. https://doi.org/10.1016/j.marchem.2015.10.004

Dash, P. K., Bhattacharyya, P., Roy, K. S., Neogi, S., & Nayak, A. K. (2019). Environmental constraints' sensitivity of soil organic carbon decomposition to temperature, management practices and climate change. *Ecological Indicators*, *107*, 10. https://doi.org/10.1016/j.ecolind.2019.105644

Di, X. Y., Xiao, B. H., Dong, H., & Wang, S. L. (2019). Implication of different humic acid fractions in soils under karst rocky desertification. *Catena*, *174*, 308–315. https://doi.org/10.1016/j.catena.2018.11.028

Elkhatib, E., & Hern, J. (1988). Kinetics of potassium desorption form Appalachian soils. *Soil Science*, *145*, 11–19. https://doi.org/10.1097/00010694-198801000-00002

Fellman, J., Hood, E., & Spencer, R. (2010). Fluorescence spectroscopy opens new windows into dissolved organic matter dynamics in freshwater ecosystems: A review. *Limnology and Oceanography*, *55*, 2452–2462. https://doi.org/10.4319/lo.2010.55.6.2452

Gao, J. J., Mikutta, R., Jansen, B., Guggenberger, G., Vogel, C., & Kalbitz, K. (2020). The multilayer model of soil mineral-organic interfaces-a review. *Journal of Plant Nutrition and Soil Science*, *183*, 27–41. https://doi.org/10.1002/jpln.201900530

Gao, Y., Yan, M. Q., & Korshin, G. (2015). Effects of calcium on the chromophores of dissolved organic matter and their interactions with copper. *Water Research*, *81*, 47–53. https://doi.org/10.1016/j.watres.2015.05.038

Gu, W. L., Huang, S. B., Lei, S., Yue, J., Su, Z. X., & Si, F. (2019). Quantity and quality variations of dissolved organic matter (DOM) in column leaching process from agricultural soil: Hydrochemical effects and DOM fractionation. *Science of the Total Environment*, *691*, 407–416. https://doi.org/10.1016/j.scitotenv.2019.07.120

Haitzer, M., Hoss, S., Traunspurger, W., & Steinberg, C. (1998). Effects of dissolved organic matter (DOM) on the bioconcentration of organic chemicals in aquatic organisms: A review. *Chemosphere*, *37*, 1335–1362. https://doi.org/10.1016/s0045-6535(98)00117-9

Han, G. L., Tang, Y., & Tan, Q. (2008). Geochemical composition of rainwater in karst forest: Case study of Maolan nature Reserve, Guizhou Province. *Bulletin of Mineralogy, Petrology and Geochemistry*, *27*(4), 363–368. https://kns.cnki.net/kcms/detail/detail.aspx?FileName=KYDH200804009&DbName=CJFQ2008

Han, Y. S., & Tokunaga, T. K. (2014). Calculating carbon mass balance from unsaturated soil columns treated with CaSO4-minerals: Test of soil carbon sequestration. *Chemosphere*, *117*, 87–93. https://doi.org/10.1016/j.chemosphere.2014.05.084

He, T., Yu, Y., Meng, Y., Su, T., Hu, J., Du, H., Wang, J., Li, Z., Zhang, Y., Wei, C., & Fan, S. (2019). Profile distribution characteristics of organic carbon and nutrients in different degraded lime soils in karst area, Northwest Guangxi Province. *Research of Soil and Water Conservation*, *26*(4), 13–18. http://stbcyj.paperonce.org/oa/DArticle.aspx?type=view&id=20190403

Helms, J., Stubbins, A., Ritchie, J., Minor, E., Kieber, D., & Mopper, K. (2007). Absorption spectral slopes and slope ratios as indicators of

molecular weight, source, and photobleaching of chromophoric dissolved organic matter. *Limnology and Oceanography*, *53*, 955–969. https://doi.org/10.2307/40058211

Henderson, R., Baker, A., Murphy, K., Hambly, A., Stuetz, R., & Khan, S. (2009). Fluorescence as a potential monitoring tool for recycled water systems: A review. *Water Research*, *43*, 863–881. https://doi.org/10.1016/j.watres.2008.11.027

Inyang, H., Onwawoma, A., & Bae, S. (2016). The Elovich equation as a predictor of lead and cadmium sorption rates on contaminant barrier minerals. *Soil & Tillage Research*, *155*, 124–132. https://doi.org/10.1016/j.still.2015.07.013

Ishii, S., & Boyer, T. (2012). Behavior of reoccurring PARAFAC components in fluorescent dissolved organic matter in natural and engineered systems: A critical review. *Environmental Science & Technology*, *46*, 2006–2017. https://doi.org/10.1021/es2043504

Judd, K. E., Crump, B. C., & Kling, G. W. (2006). Variation in dissolved organic matter controls bacterial production and community composition. *Ecology*, *87*, 2068–2079. https://doi.org/10.1890/0012-9658(2006)87[2068:vidomc]2.0.co;2

Kaiser, K. (1998). Fractionation of dissolved organic matter affected by polyvalent metal cations. *Organic Geochemistry*, *28*, 849–854. https://doi.org/10.1016/s0146-6380(98)00046-1

Kalbitz, K., Solinger, S., Park, J. H., Michalzik, B., & Matzner, E. (2000). Controls on the dynamics of dissolved organic matter in soils: A review. *Soil Science*, *165*, 277–304. https://doi.org/10.1097/00010694-200004000-00001

Kerr, J., & Eimers, C. (2012). Decreasing soil water Ca^{2+} reduces DOC adsorption in mineral soils: Implications for long-term DOC trends in an upland forested catchment in southern Ontario, Canada. *The Science of the Total Environment*, *427-428*, 298–307. https://doi.org/10.1016/j.scitotenv.2012.04.016

Kim, H. S., Kim, K. R., Lee, S. H., Kunhikrishnan, A., Kim, W. I., & Kim, K. H. (2018). Effect of gypsum on exchangeable sodium percentage and electrical conductivity in the Daeho reclaimed tidal land soil in Korea—A field scale study. *Journal of Soils and Sediments*, *18*, 336–341. https://doi.org/10.1007/s11368-016-1446-x

Kowalczuk, P., Durako, M. J., Young, H., Kahn, A. E., Cooper, W. J., & Gonsior, M. (2009). Characterization of dissolved organic matter fluorescence in the South Atlantic Bight with use of PARAFAC model: Interannual variability. *Marine Chemistry*, *113*, 182–196. https://doi.org/10.1016/j.marchem.2009.01.015

Kretzschmar, R., & Sticher, H. (1997). Transport of humic-coated iron oxide colloids in a sandy soil: Influence of Ca^{2+} and trace metals. *Environmental Science & Technology*, *31*, 3497–3504. https://doi.org/10.1021/es970244s

Lal, R. (2005). Soil erosion and dynamics. *Soil and Tillage Research*, *81*, 137–142. https://doi.org/10.1016/j.still.2004.09.002

Lechleitner, F. A., Dittmar, T., Baldini, J. U. L., Prufer, K. M., & Eglinton, T. I. (2017). Molecular signatures of dissolved organic matter in a tropical karst system. *Organic Geochemistry*, *113*, 141–149. https://doi.org/10.1016/j.orggeochem.2017.07.015

Liu, F., Wang, S. J., Luo, H. B., Liu, Y. S., He, T. B., & Long, J. (2006). Vegetation succession with karst rocky desertification and its impaction on water chemistry of runoff. *Acta Pedologica Sinica*, *43*(1), 26–32. https://doi.org/10.11766/trxb200411260104

Münch, J. M., Totsche, K., & Kaiser, K. (2002). Physiochemical factors controlling the release of dissolved organic carbon from columns of forest subsoils. *European Journal of Soil Science*, *53*, 311–320. https://doi.org/10.1046/j.1365-2389.2002.00439.x

Oren, A., & Chefetz, B. (2012). Sorptive and desorptive fractionation of dissolved organic matter by mineral soil matrices. *Journal of Environmental Quality*, *41*, 526–533. https://doi.org/10.2134/jeq2011.0362

Pifer, A. D., Miskin, D. R., Cousins, S. L., & Fairey, J. L. (2011). Coupling asymmetric flow-field flow fractionation and fluorescence parallel factor analysis reveals stratification of dissolved organic matter in a drinking water reservoir. *Journal of Chromatography A*, *1218*, 4167–4178. https://doi.org/10.1016/j.chroma.2010.12.039

Qualls, R. G., & Haines, B. L. (1991). Geochemistry of dissolved organic nutrients in water percolating through a forest ecosystem. *Soil Science Society of America Journal*, *55*, 1112–1123. https://doi.org/10.2136/sssaj1991.03615995005500040036x

Rashad, M., Dultz, S., & Guggenberger, G. (2010). Dissolved organic matter release and retention in an alkaline soil from the Nile River delta in relation to surface charge and electrolyte type. *Geoderma*, *158*, 385–391. https://doi.org/10.1016/j.geoderma.2010.06.007

Reemtsma, T., Bredow, A., & Gehring, M. (1999). The nature and kinetics of organic matter release from soil by salt solutions. *European Journal of Soil Science*, *50*, 53–64. https://doi.org/10.1046/j.1365-2389.1999.00212.x

Schaumann, G. (1999). Effect of $CaCl_2$ on the kinetics of dissolved organic matter release from a sandy soil. *Journal of Plant Nutrition and Soil Science*, *163*, 523–529. https://doi.org/10.1002/1522-2624(200010)163:53.0.CO;2-J

Scott, E., & Rothstein, D. (2014). The dynamic exchange of dissolved organic matter percolating through six diverse soils. *Soil Biology and Biochemistry*, *69*, 83–92. https://doi.org/10.1016/j.soilbio.2013.10.052

Setia, R., Rengasamy, P., & Marschner, P. (2013). Effect of exchangeable cation concentration on sorption and desorption of dissolved organic carbon in saline soils. *Science of the Total Environment*, *465*, 226–232. https://doi.org/10.1016/j.scitotenv.2013.01.010

Shabarova, T., Villiger, J., Morenkov, O., Niggemann, J., Dittmar, T., & Pernthaler, J. (2014). Bacterial community structure and dissolved organic matter in repeatedly flooded subsurface karst water pools. *FEMS Microbiology Ecology*, *89*, 111–126. https://doi.org/10.1111/1574-6941.12339

Singh, S., D'Sa, E., & Swenson, E. (2010). Chromophoric dissolved organic matter (CDOM) variability in Barataria basin using excitation-emission matrix (EEM) fluorescence and parallel factor analysis (PARAFAC). *Science of the Total Environment*, *408*, 3211–3222. https://doi.org/10.1016/j.scitotenv.2010.03.044

Stedmon, C., & Bro, R. (2008). Characterizing dissolved organic matter fluorescence with parallel factor analysis: A tutorial. *Limnology and Oceanography*, *6*, 572–579. https://doi.org/10.4319/lom.2008.6.572

Stedmon, C., & Markager, S. (2005). Resolving the variability in dissolved organic matter fluorescence in a temperate estuary and its catchment using PARAFAC analysis. *Limnology and Oceanography*, *50*, 686–697. https://doi.org/10.4319/lo.2005.50.2.0686

Stutter, M., Lumsdon, D., & Thoss, V. (2006). Physico-chemical and biological controls on dissolved organic matter in peat aggregate columns. *European Journal of Soil Science*, *58*, 646–657. https://doi.org/10.1111/j.1365-2389.2006.00851.x

Sumner, M. E., & Miller, W. P. (1996). Cation exchange capacity and exchange coefficients. In D. Sparks, A. Page, P. Helmke, R. Loeppert, P. N. Soltanpour, M. A. Tabatabai, C. T. Johnston and M. E. Sumner, (Eds.), *Methods of Soil Analysis*. https://doi.org/10.2136/sssabookser5.3.c40

Tang, H. M., Xiao, B. H., & Xiao, P. W. (2021). Interaction of Ca^{2+} and soil humic acid characterized by a joint experimental platform of potentiometric titration, UV–visible spectroscopy, and fluorescence spectroscopy. *Acta Geochimica*, *40*, 300–311. https://doi.org/10.1007/s11631-021-00453-7

Tang, H. Y., Liu, Y., Li, X. M., Muhammad, A., & Huang, G. Q. (2019). Carbon sequestration of cropland and paddy soils in China: Potential, driving factors, and mechanisms. *Greenhouse Gases: Science and Technology*, *9*, 872–885. https://doi.org/10.1002/ghg.1901

Tavakkoli, E., Rengasamy, P., Smith, E., & McDonald, G. (2015). The effect of cation-anion interactions on soil pH and solubility of organic carbon. *European Journal of Soil Science*, *66*, 1054–1062. https://doi.org/10.1111/ejss.12294

Tiemeyer, B., Pfaffner, N., Frank, S., Kaiser, K., & Fiedler, S. (2017). Pore water velocity and ionic strength effects on DOC release from peat-sand mixtures: Results from laboratory and field experiments. *Geoderma*, *296*, 86–97. https://doi.org/10.1016/j.geoderma.2017.02.024

Tipping, E., Berggren, D., Mulder, J., & Woof, C. (1995). Modeling the solid-solution distributions of protons, aluminum, base cations and humic substances in acid soils. *European Journal of Soil Science*, *46*, 77–94. https://doi.org/10.1111/j.1365-2389.1995.tb01814.x

Tipping, E., & Hurley, M. A. (1992). A unifying model of cation binding by humic substances. *Geochimica et Cosmochimica Acta*, *56*, 3627–3641. https://doi.org/10.1016/0016-7037(92)90158-f

van de Weert, M. (2010). Fluorescence quenching to study protein-ligand binding: Common errors. *Journal of Fluorescence*, *20*, 625–629. https://doi.org/10.1007/s10895-009-0572-x

Wang, S. J., Liu, M., & Zhang, D. F. (2004). Karst rocky desertification in southwestern China: Geomorphology, landuse, impact and rehabilitation. *Land Degradation & Development*, *15*, 115–121. https://doi.org/10.1002/ldr.592

Weishaar, J. L., Aiken, G. R., Bergamaschi, B. A., Fram, M. S., Fujii, R., & Mopper, K. (2003). Evaluation of specific ultraviolet absorbance as an indicator of the chemical composition and reactivity of dissolved organic carbon. *Environmental Science & Technology*, *37*, 4702–4708. https://doi.org/10.1021/es030360x

Xiao, P. W., & Xiao, B. H. (2021). Research progress of soil column leaching experiment and its application prospect in soil organic carbon migration. *Earth and Environment*, *49*(1), 106–114. https://doi.org/10.14050/j.cnki.1672-9250.2020.48.096

Zhang, P., Hu, X., Yang, H., Ren, M., Zhou, M., & Chen, L. (2020). Characteristics of soil calcium forms of rocky desertification areas in the Mengzi fault-depression basin, Yunnan. *Carsologica Sinica*, *39*(3), 368–374. http://zgyr.karst.ac.cn/ch/reader/view_abstract.aspx?file_no=20200310&flag=1

Zhou, C. S., Zou, S. Z., Zhu, D. N., Xie, H., Chen, H. F., & Yu, J. G. (2017). Contrast study of Ca^{2+} and HCO3- concentration in karst-water samples between field test and laboratory test values. *Carsologica Sinica*, *36*(5), 684–690. http://zgyr.karst.ac.cn/ch/reader/view_abstract.aspx?file_no=20170511&flag=1

Zsolnay, Á. (2003). Dissolved organic matter: Artefacts, definitions, and functions. *Geoderma*, *113*, 187–209. https://doi.org/10.1016/S0016-7061(02)00361-0

SUPPORTING INFORMATION

Additional supporting information may be found in the online version of the article at the publisher's website.

How to cite this article: Xiao, P., Xiao, B., & Adnan, M. (2021). Effects of Ca^{2+} on migration of dissolved organic matter in limestone soils of the southwest China karst area. *Land Degradation & Development*, *32*(17), 5069–5082. https://doi.org/10.1002/ldr.4092